Spectroscopic Studies of Cds Nanoparticles Synthesized by RF-Magnetron Sputtering Technique

P. K. Ghosh
Dept of Physics
Abhedananda Mahavidyalaya, Sainthia, Birbhum, W.B, India

Abstract- *Nanoparticles of CdS have been produced by rf-sputtering method. X-ray diffraction patterns and selected area electron diffraction patterns confirmed the nanocrystalline cubic CdS phase formation. TEM measurements of the CdS thin film prepared on carbon coated copper grid show that the particle size lies in the range 2 - 5 nm and the optical transmittance measurement shows above 85 % transparency in the wavelength range 500 - 800 nm. Effects of electrodes distance variation on the optical properties of the nanoparticles were studied. The direct optical bandgap value of the films initially decreased with lowering of electrode distance then increased. The direct optical bandgap lies in the range 3.09 eV to 3.67 eV and indirect bandgap 1.74 eV to 3.18 eV for electrode distance variation 2 cm to 4 cm.*

Keywords- nanoparticles, rf-sputtering, electrode distance, optical properties

I. INTRODUCTION

Nanostructured materials have gained special interest in recent years due to their new properties providing the theoretical concepts [1-3] in physics associated with it. Quantum confinement effects are observed in nanoparticles because of large surface to volume ratio, resulting in high density of surface states. Preparation and study of nanoparticles[4,5], nanobelts [6,7], nanofibres and nanowires [8,9] have been reported by different groups with different routes. One-dimensional nanostructured materials have gained immense importance in the assembly of nanodevices [10,12]. Nanometer-scale electronics have opened the new area of application in device technology[13]. One-dimensional nanoscale materials may be utilized in various nanodevices including nanologic circuits, nanolasers, nanosensers, nanothermometers[14], etc. Quantum wires of semiconductors [15] and metallic alloys [16] have found to exhibit interesting magnetic and electrical properties.

Quantum confinement effect modifies the electronic structure of nanocrystals when the sizes of the nanoparticles are comparable to that of Bohr excitonic radius of those materials. Hence depending upon the sizes of the materials, the nanoscale semiconductors show interesting properties, and great efforts have been imposed on controlling their sizes. Starting from the zero-dimensional nanoparticles, various structures, such as nanowires, nanorods, nanotubes and nanobelts have been produced from different materials [17-20], among them CdS is one of the widely studied materials. Previously, CdS nanowires have been reported via chemical bath deposition process by Zhang et al [21]. CdS nanoparticles have been prepared via sol-gel method by Mathieu et al [22]. Murray et al[23] and Counio et al[24] have synthesized CdS nanoparticles by pyrolysis of organometalic reagents and controlling precipitation of nanocrystals in inverted micelles respectively. CdS nanoparticles embedded in silicon dioxide matrix have also been reported via magnetron rf-sputtering technique by Rolo et al[25] and Vasileviskiy et al. Recently, CdS nanoparticles have been grown within the self-organized pores of a polymer matrix via chemical bath deposition by us [26]. As the nanoscale semiconductors show interesting properties [27-30], different properties of CdS thin films studied by different groups [31-32]. In this paper we have reported the synthesis and characterizations of CdS nanoparticles by rf-magnetron sputtering without any capping agents or matrix.

II. EXPERIMENTAL

2.1 Target preparation for sputtering

Cadmium sulphide (CdS) target was fabricated by taking a suitable aluminium holder (2 inch dia) and compacting the hexagonal CdS polycrystalline powder by applying suitable hydrostatic pressure (~ 100 kg / cm^2). The fabricated CdS target was placed in the radio frequency magnetron-sputtering chamber for the deposition of nanocrystalline thin films on various substrates such as glass and Si.

2.2 Film synthesis

The films were synthesized at room temperature and the substrate used was glass and Si. The glass substrates were cleaned at first by a mild soap solution, then in boiling water and ultrasonic cleaner and finally degreased in alcohol vapor.

For Si substrates, to remove the surface oxide layer, they were etched in HF (~20%) for 5 minutes and finally cleaned in an ultrasonic cleaner. The chamber was evacuated by conventional rotary and diffusion pump combination to a base pressure of 10^{-6} mbar. Before starting the actual deposition the target was pre-sputtered and the substrates were covered by a movable shutter. The working pressure of the evacuated chember was maintained at ~ 0.08 mbar sending argon gas during deposition of the film. The sputtering was performed at varying the target to substrate distance from 1.5 cm to 4 cm keeping constant rf power at 260 watt. For transmission electronic measurement the films were directly deposited on carbon coated copper grid.

2.3 Characterization

The deposited films were characterized by studying mainly structural and optical properties. UV-VIS spectrophotometric measurement was performed by using a spectrophotometer (Shimadzu UV-3101PC) at room temperature. The spectrum was recorded by taking a similar glass as reference and hence transmission due to the film only was obtained. For phase confirmation an X-ray diffractometer (Bruker Advance D8) was used. XRD pattern was measured in 2θ range 20 - 70 ^{o} using Cu K□ radiation of wavelength □= 0.15406 nm. For TEM measurement a transmission electron microscope (Hitachi 600) was used. The details of the characterizational result are discussed in the following.

III. RESULTS AND DISCUSSION

3.1 X- Ray Diffraction and Nanostructural studies

X-ray diffraction pattern of CdS powder (target material) and thin films were studied. The several peaks of hexagonal phase of CdS powder with a = b = 4.136 Å, c = 6.713 Å, have been obtained due to diffraction form (100), (002), (111), (102), (110), (103), (112) and (203) planes of CdS as shown in Fig.1. For thin films, only the reflection from (111) plane of cubic CdS (a_0 = 5.818 Å = b_0 = c_0). Fig.2 shows the XRD spectra of CdS thin films for target to substrate distances (a) 4 cm, (b) 3.5 cm, (c) 3 cm and (d) 2.5 cm. Also the peaks are broadened due to the nanocrystallinity of the films. Here it should also be noted that the broadening of peak increases with the increase in electrode distance and bellow electrode distance 2 cm quality of deposited film is not so good. The information on strain (ε) and the crystallite size (L) of CdS thin films have been obtained from the following Debye-Scherrer relations:

$$L = \lambda / \beta \cos\theta \quad \text{and} \quad s = \beta / 4\tan\theta \qquad (1)$$

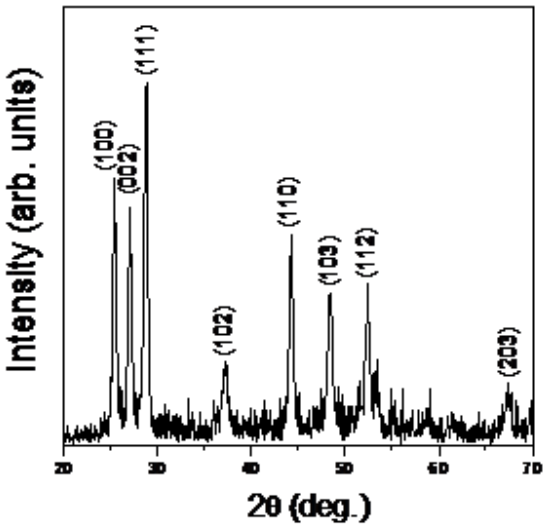

Figure 1: XRD pattern of CdS powder of the target Material.

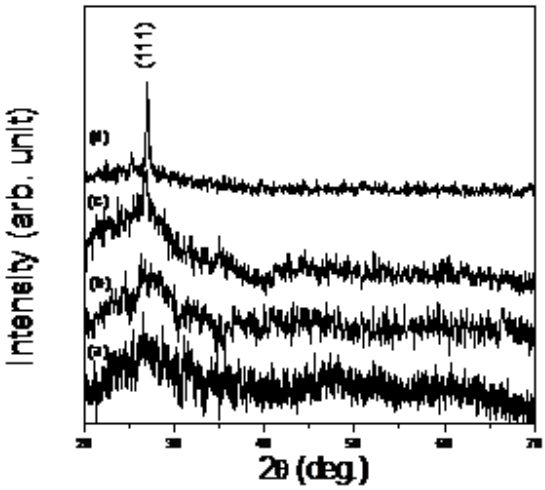

Figure 2: XRD patterns of CdS thin films for different electrode distances.

where β is the Full-Widths-at-Half-Maximum (FWHM) of the diffraction peaks. Inset of The interplaner spacing (d) corresponding to XRD peaks, TEM measurement and JCPDS data card [33] have been computed as shown in table 1. The variation of crystallite size and strain with electrode distance are shown in Fig.3. From this figure, it is clear that the crystallite size decreases and strain increases with the increase in substrate to target distance.

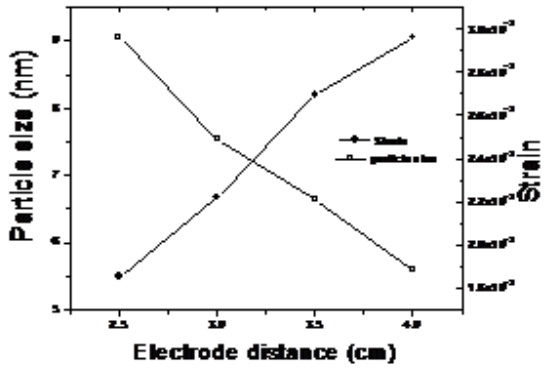

Figure 3: Variation of particle size and strain with different electrode distance

Table 1. Interplaner spacing (d) from TEM, XRD, JCPDS files corresponding (hkl) values.

$d_{(TEM)}$ Å	$d_{(XRD)}$ Å	$d_{(JCPDS)}$ Å	(hkl)
3.123	3.123	3.123	(111)
2.761		2.765	(200)
1.912		1.912	(220)
1.632		1.633	(311)

The nanostructured of the films, deposited on carbon coated copper grid, were studied at room temperature by using a transmission electron microscope (TEM). The micrographs and corresponding diffraction pattern of CdS nanoparticles have been shown in Fig. 4 (a) and (b) respectively. The presence of CdS nanoparticles is clearly visible in TEM picture and corresponding diffraction pattern of the film consists of central halo and concentric rings. From the diameter of the rings, we calculate the inter-planer spacing (d) values, which correspond to reflection from (111), (220) and (311) planes of cubic CdS with a_0 = 5.4060 Å. From TEM micrograph we obtained the diameter of the particles lies in the range of 2 nm to 4.35 nm.

3.2 Optical absorption and optical bandgap

The bandgap of the film $E_{g(film)}$ was determined from the transmission vs. wavelength traces (as shown in Fig.5 for variation of electrode distance) recorded in the range 300 - 800 nm. These show above 85 % transmittance in the wavelength range of 550 nm to 800 nm. The fundamental absorption, which corresponds to electron excitation from the valance band to conduction band, can be used to determine the nature and value of the optical band gap. The relation between the absorption coefficients ((α) and the incident photon energy (hν)can be written as [34],

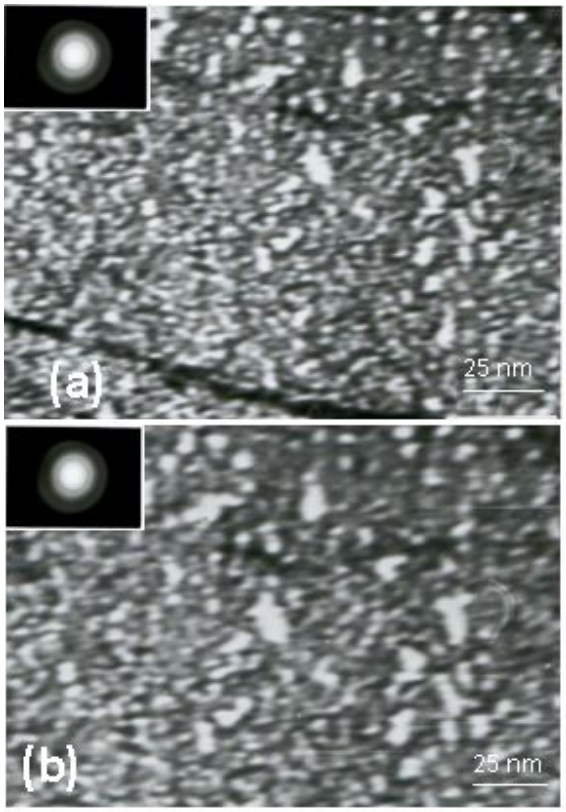

Figure 4: (a) and (b) TEM micrographs for electrode distances 3.5 cm and 3 cm respectively, Inset: Selected area electron diffraction pattern of CdS thin film deposited on carbon coated copper grid.

$$(\alpha h\nu)^{1/n} = A(h\nu - E_g) \qquad (2)$$

where A is a constant and E_g is the band gap of the material and exponent n depends on the type of transition. For direct allowed n=1/2 , indirect allowed transition, n=2, and for direct forbidden, n=3/2. To determine the possible transitions, $(\alpha h\nu)^{1/n}$ vs. hν were plotted and corresponding band gap were obtained from extrapolating the straight portion of the graph on hν axis. The direct bandgaps (lie in the range 3.09 eV to 3.67 eV) and indirect bandgaps (lie in the range 1.74 eV to 3.18 eV) calculated from $(\alpha h\nu)^2$ vs. hν and $(\alpha h\nu)^{1/2}$ vs. hν plots respectively are shown in Fig.6 and Fig.7 for substrate to target distance variation from 2 cm to 4 cm. The direct bandgap values of the films are higher than that of bulk value of CdS (2.42 eV) because of quantum confinement of carriers in CdS nanocrystals.

The properties of nanocrystalline materials change from their corresponding bulk properties due to the sizes of the nanoparticles become less or comparable to the Bohr excitonic radius (r_B).

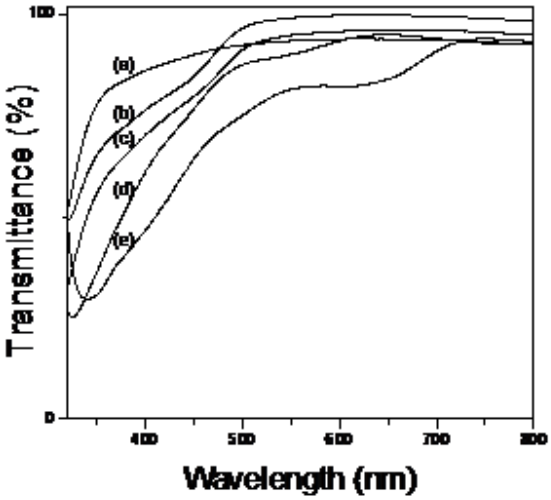

Figure 5: Transmittance vs. wavelength plot of nanocrystalline CdS thin film for different electrode distance.

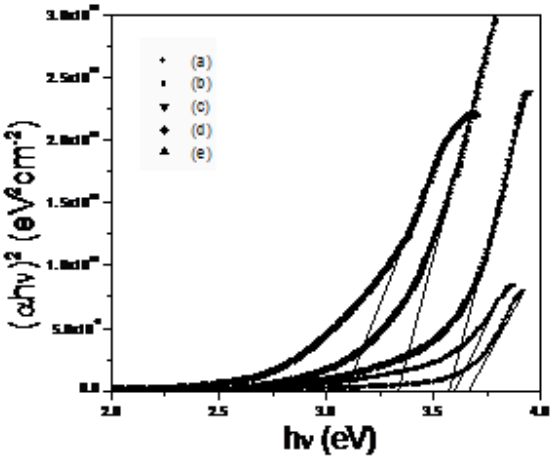

Figure 6: Plot to determine direct bandgap of the CdS thin film for different electrode distances.

$$r_B = h^2 \varepsilon [1/m^*_e + 1/m^*_h] / \pi e^2 \quad (3)$$

where ε is the permittivity of the sample, m^*_e = $0.21m_0$ and m^*_h = $0.80m_0$ are the effective mass of electron and hole in CdS respectively, where m_0 is the mass of a free electron. From the above relation the Bohr radius of CdS comes out as 2.8 nm. The values of particle sizes in the nanocrystalline CdS thin film, as determined from that of TEM studies, are comparable to Bohr radius supporting the quantum size effect.

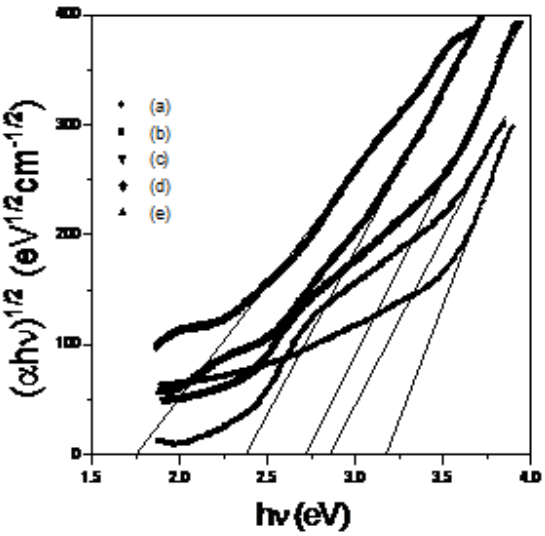

Figure 7: Plot to determine indirect bandgap of the thin film for different electrode

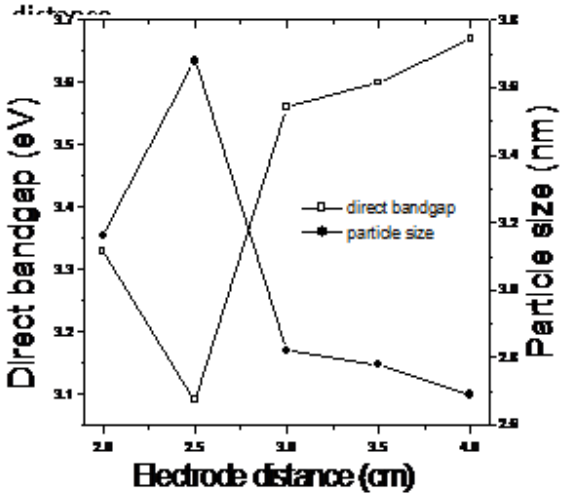

Figure 8: Variation of optical bandgap and particle size with electrode distances

The shift of band gap might also be utilized in determining the crystal radius (r) using relation [35, 36]

$$\Delta E_g = E_{g(nm)} - E_{g(bulk)} = [h^2 / 8\mu r^2] - [1.8\, e^2 / r\varepsilon] \quad (4)$$

where μ is the reduced mass of electron-hole effective masses and ε is the dielectric constant. The particle sizes have been calculated from above relation and those lie in the range 2.69 nm to 3.68 nm for variation of electrode distance. The same obtained from TEM measurement also fairly support these results.

Table II: Comparison of electrode distance, direct bandgap, indirect bandgap and particle size from shift of direct bandgap.

Name of the sample	Electrode distance (cm)	Direct bandgap (eV)	Indirect bandgap (eV)	Crystallite size (nm)
(a)	4.0	3.67	3.18	2.69
(b	3.5	3.60	2.85	2.78
(c)	3.0	3.56	2.72	2.82
(d)	2.0	3.33	2.37	3.16
(e)	2.5	3.09	1.74	3.68

The variation of direct bandgap and particle size (obtained from the shift of bandgap to that of bulk value) with electrode distance are shown in Fig.8. It is clear from the figure that the particle size increases (3.16 nm to 3.68 nm) with the increase of electrode distance (2 cm to 2.5 cm) first and then it decreases (3.68 nm to 2.69 nm) with the increase of electrode distance (2.5 cm to 4 cm).

IV. CONCLUSIONS

The thin films of CdS nanoparticles, deposited by rf-magnetron sputtering were well dispersed. TEM and optical studies revealed that the quantum size effect was predominant in determining the above properties with particle size lying in the range 2 nm to 4.35 nm. XRD study revealed the cubic phase of nanocrystalline CdS. Optical transmission spectrum showed above 80 % transmittance in the wavelength range of 450 nm to 800 nm and a high direct bandgap 3.81 eV to 2.90 eV and indirect bandgap was also high due to quantum confinement effect in CdS.

V. ACKNOWLEDGEMENT

The author wishes to thank Prof. K. K. Chattopadhyay of Thin Film Nanoscience Laboratory, Jadavpur University Kolkata, for all types of supports during the execution of the work.

REFERENCES

[1] A. J. Cox, J. G. Louderback, and L. A. Bloomfield, Phys Rev. Lett. 71, 923 (1993).
[2] J. R. Heath, Science 270, 1315 (1995).
[3] A. P. Alivisatos, Science 271, 933 (1996).
[4] A.Lorke, J. P. Kotthaus, and K. Ploog, Phys. Rev. Lett.64, 2559 (1990).
[5] T. Demel, D. Heitmann, P. Grambow and K. Ploog, Phys. Rev. Lett. 64, 2559 (1990).
[6] Y. C. Zhu, Y. Bando and D. F. Xue, Appl. Phys. Lett. 82, 1769 (2003).
[7] Q. Li and C. Wang, Appl. Phys. Lett. 83, 359 (2003).
[8] T. Egeler, G. Abstreiter, G. Weimann, T. Demel, D. Heitmaann, P. Grambow, Phys. Rev. Lett. 65, 1804 (1990).
[9] T. Demel, D. Heitmann, P. Grambow and K. Ploog, Phys. Rev. Lett. 66, 2657 (1991).
[10] Y. Huang, X. F. Duan, Q. Q. Wei, and C. M. Lieber, Science 291, 851 (2001).
[11] A. Bachtold, P. Hadley, T. Nakanishi and C. Dekker, Science 294, 1317 (2001).
[12] M. H. Huang, S. Mao, H. Feick, H. Q. Yan, Y. Y. Wu, H. Kind, E. Weber, R. Russo and P. D. Yang, Science 292, 1897 (2001).
[13] R. F. Pease, in Nanostructures and mesoscopic systems, edited by W. P. Kirk and M. A. Reed (Academic, NewYork, 1992), p. 37.
[14] Y. Q. Gao and Y. Bando, Nature 415, 599 (2002).
[15] S. T. Lee, Y. F. Zhang, N. Wang, Y. H. Tang, I. Bello, C. S. Lee, and Y. W. Chung, J. Mater. Res. 14, 4503 (1993).
[16] H. J. Blythe, V. M. Fedosynk, O. I. Kasyutich, and W. Schwarzacher, J. Magn. Magn. Matter. 208, 251 (2000).
[17] S. Lijima and T. Ichihashi, Nature 36, 603 (1993).
[18] Z. W. Pan, Z. R. Dai and Z. L. Wang, Science 291, 1947 (2001).
[19] Y. C. Zhu, H. L. Li, Y. Koltypin, Y. R. Hacohen and A. Gedanken, Chem. Commun. 24, 2616 (2001).
[20] Y. H. Gao, Y. Bando and T. Salo, Appl. Phys. Lett. 79, 4565 (2001).
[21] H. Zhang, X. Ma, J. Xu, J. Niu, J. Sha and D. Yang,J. Cryst. Growth 246, 108 (2002).
[22] H. Mathieu, T. Richard, J. Allegre, P. Lefebvre, G. Arnaud, W. Granier, L. Boudes, J. L. Marc, A. Pradel and M. Ribes, J. Appl. Phys. 77, 287 (1994).
[23] C. B. Murray, D. J. Norris and M. G. Bawendi, J. Am. Chem. Soc. 115, 8706 (1993).
[24] G. Counio, S. Esnouf, T. Gacoin and J. P. Boilot, J. Phys. Chem. 100, 20021 (1996).
[25] A.G. Rolo, O. Conde and M. J. M. Gomes, Thin Solid Films 318, 108 (1998).
[26] P. K. Ghosh, R. Maity, K. K. Chattopadhyay, J. Nanoscience & Nanotechnology, Vol. 5, 1–6, (2005)
[27] J. Bahadur, S. Agrawal, V. Panwar, A. Parveen, K. Pal, Macromolecular Research. 1–6 (2016).
[28] S. Agrawal, A. Parveen, A. Azam, Mater. Lett. 168 125–128 (2016).
[29] S. Agrawal, A. Parveen, A. Azam, J. Magn. Magn. Mater. 414 144–152 (2016).
[30] R.K. Duchaniya, Int. J. Mining, Metall. Mech. Eng. 2, 54–56 (2014).z
[31] A. Hasnat and J. Podder Journal Scientific Research, 4 (1), 11-19 (2012)

[32] M. Penchal Reddy1*, B.C. Jamalaiah2, I.G. Kim1, D.S. Yoo1, K.V. Siva Kumar3, R. Ramakrishna Reddy, Adv. Mat. Lett. 4(8), 621-625 (2013).
[33] J.C.P.D.S. Powder Diffraction File Card 10 - 454.
[34] I. C. Pankove, Optical Processes in Semiconductors, Prentice-Hall.Inc., (1971).
[35] Y. S. Yuang, F. Y. Chen, Y. Y. Lee and C. L. Liu, Jpn. J. Appl. Phys. 76, 3041
(1994).
[36] A.D. Yoffe, Adv. In Phys. 42, 173 (1993).